

Tomography of exotic hadrons in high-energy exclusive processes

H. Kawamura¹ and S. Kumano^{1,2}

¹*KEK Theory Center, Institute of Particle and Nuclear Studies
High Energy Accelerator Research Organization (KEK)*

1-1, Ooho, Tsukuba, Ibaraki, 305-0801, Japan

²*J-PARC Branch, KEK Theory Center, Institute of Particle and Nuclear Studies, KEK
and Theory Group, Particle and Nuclear Physics Division, J-PARC Center*

203-1, Shirakata, Tokai, Ibaraki, 319-1106, Japan

(Dated: January 23, 2014)

We investigated the possibility of determining internal structure of exotic hadrons by using high-energy reaction processes, where quarks and gluons are appropriate degrees of freedom. In particular, it should be valuable to investigate the high-energy exclusive processes which include generalized parton distributions (GPDs) and generalized distribution amplitudes (GDAs). The GPDs and GDAs contain momentum distributions of partons and form factors. We found that the exotic nature appears in momentum distributions of quarks as suggested by the constituent-counting rule and in the form factors associated with exotic hadron sizes and the number of constituents. Transition GPDs to exotic hadrons could probe such exotic signatures. We also propose that these exotic signatures should be found in exclusive production processes of exotic hadrons from $\gamma^*\gamma$ in electron-positron annihilation. For example, the GDAs contain information on a time-like form factor of the energy-momentum tensor of a hadron h . We show that the cross section of $e\gamma \rightarrow e + h\bar{h}$ is sensitive to the exotic signature by looking at the $h\bar{h}$ invariant-mass dependence by taking light hadrons, $h = f_0(980)$ and $a_0(980)$. From such GDA measurements, the tomography of exotic hadrons becomes possible, for example, by Belle and BaBar experiments and by future linear collider.

PACS numbers: 13.66.Bc, 12.39.Mk

I. INTRODUCTION

Almost a half century has passed since the original quark model was proposed by Gell-Mann and Zweig in 1964. The model suggested that hadrons are classified into two categories, baryons with three quarks and mesons with a quark and an antiquark. Although there were speculations on other hadron configurations, such as tetra-quark hadrons of the $qq\bar{q}\bar{q}$ configuration and penta-quark hadrons of $qqqq\bar{q}$, which are not forbidden by the fundamental theory of strong interactions, quantum chromodynamics (QCD), it is rather surprising that such exotic hadrons have not been found undoubtedly for a long time [1].

We are, however, fortunate to start observing some precursory signatures of exotic hadrons, for example $Z(4430)$, after so many years of theoretical and experimental investigations [2]. There are reports on new findings on heavy hadrons with charm and bottom quarks [3]. However, even in the low-mass region of 1 GeV, there are controversial hadrons $f_0(980)$ and $a_0(980)$ which could be tetra-quark (or $K\bar{K}$ molecule) hadrons [4, 5, 6], and $\Lambda(1405)$ which could be a penta-quark (or $\bar{K}N$ molecule) hadron [7]. However, internal structure of exotic hadrons is not easily determined by low-energy measurements on global properties such as masses and decay widths. Since similar masses and decay widths could be obtained in ordinary hadron pictures, it is rather difficult to entangle various possibilities on internal configurations.

We propose that internal configurations of exotic-hadron candidates can be determined by high-energy re-

actions, especially exclusive processes. It is particularly noteworthy that quark and gluon degrees of freedom appear in the high-energy reactions. Therefore, it is appropriate to use high-energy exclusive processes for determining the internal structure of exotic hadrons. There was a proposal to use fragmentation functions for finding the exotic nature by noting the characteristic differences between favored and disfavored fragmentation functions depending on an internal quark configuration [8]. For example, the fragmentation functions of an exotic-hadron candidate $f_0(980)$ could be measured by the KEK-B factory [9]. We also proposed that the constituent-counting rule in hard exclusive processes should be useful for determining the number of active constituents in exotic hadrons by taking $\Lambda(1405)$ production as an example [10]. There are also studies on exotic hadrons by hard electro-production processes [11]. Such theoretical and experimental studies have not been extensively explored yet at high energies although it could be considered to be a promising future direction of exotic-hadron studies.

On the other hand, internal structure of the nucleon becomes a new area recently in investigating transverse configuration in addition to the longitudinal partonic structure. It is the field of ‘‘hadron tomography’’ to find the three-dimensional (3D) structure of hadrons. It partly originates from the nucleon-spin puzzle in the sense that transverse structure, namely orbital angular momenta of quarks and gluons, needs to be understood because quark and gluon spin contributions are rather small for constituting the spin 1/2 of the nucleon. These 3D picture of the nucleon has been recently investigated by transverse-momentum-dependent parton dis-

tributions (TMDs) and generalized parton distributions (GPDs) [12, 13, 14, 15, 16]. The TMDs, especially the unpolarized distributions, are sometimes called unintegrated parton distribution functions (uPDFs).

These distribution functions contain information on internal configuration of the nucleon. The longitudinal part contains the information of longitudinal momentum distributions of partons, and the transverse part reflects the transverse size. In this article, we show that these two ingredients could have information on exotic hadron structure if the GPDs are investigated for exotic-hadron candidates. We also suggest that generalized distribution amplitudes (GDAs), which are investigated in the s - t crossed process to the GPD one, should be appropriate quantities for determining the internal structure of exotic hadrons. Here, s and t are Mandelstam variables. The GDAs can be investigated in $\gamma^* \gamma$ collisions and there are available $e^+ e^-$ colliders in the world including the high-luminosity KEK-B factory for such GDA studies. The two-photon physics has been studied for investigating hadron properties [17], and it can be now used for the GDA studies.

This article is organized in the following way. In Sec. II, definitions of the GPDs and GDAs are explained by starting from the basic function of the Wigner distribution for a hadron. Then, possible longitudinal momentum distributions and form factors are explained for exotic hadrons. Then, the formalism is shown for calculating exclusive cross sections for $e + \gamma \rightarrow e + h + \bar{h}$ to investigate internal structure of exotic hadron candidates by the GDAs. Numerical results are shown in Sec. III, and they are summarized in Sec. IV.

II. FORMALISM

We explain the generalized parton distributions (GPDs) and generalized distribution amplitudes (GDAs) of hadrons for investigating internal structure of exotic hadron candidates. As an example of actual high-energy reaction processes, an electron-positron annihilation is explained for investigating the exotic GDAs by exclusive production processes from $\gamma^* \gamma$.

Although the GPDs and GDAs are well-known quantities for nucleon-structure physicists especially in the nucleon-spin community, they may not be very familiar in low-energy hadron-physics communities. Therefore, we provide the following introductory explanations on the Wigner distributions, GPDs, and GDAs in Secs. II A, II B, and II C, respectively. Our work is to connect the GPDs and GDAs with the exotic-hadron studies by the forms of momentum distributions of partons, form factors, *etc.*, and they are explained in Secs. III B, III C, and III D.

A. Wigner distributions

Nucleon structure has been investigated mainly by the form of deep-inelastic structure functions and elastic form factors. The structure functions indicate longitudinal momentum distributions of partons. In high-energy hadron reactions, only longitudinal degrees of freedom are usually focused by integrating the transverse components. However, transverse degrees of freedom are becoming increasingly important nowadays, for example, in clarifying the origin of the nucleon spin by orbital angular momenta of partons and in describing hadron-production processes at hadron colliders such as RHIC (Relativistic Heavy Ion Collider), Tevatron, and LHC (Large Hadron Collider) by including the transverse-momentum dependent parton distributions. Therefore, the GPDs, TMDs, and uPDFs are now under extensive and systematic investigations as one of major projects in hadron physics [12, 13]. These quantities originate from the Wigner distribution for the nucleon. In one-dimensional quantum mechanics, the Wigner distribution is defined by

$$W(x, p) = \int d\xi e^{ip\xi/\hbar} \psi^*(x - \xi/2) \psi(x + \xi/2). \quad (1)$$

We consider the simple case of one-dimensional harmonic oscillator given by the Hamiltonian $H = p^2/(2m) + m\omega^2 x^2/2$. Solving the Schrödinger equation, we obtain the Wigner distribution

$$W_n(x, p) = \frac{(-1)^n}{\pi\hbar} e^{-2H/(\hbar\omega)} L_n\left(\frac{4H}{\hbar\omega}\right), \quad (2)$$

where the functions $L_n(x)$ are the Laguerre polynomials. If the classical limit is taken by $\hbar \rightarrow 0$ and $n \rightarrow \infty$, the Wigner function becomes

$$W_n(x, p) \rightarrow \delta(H(x, p) - E_n) \quad \text{as } \hbar \rightarrow 0, \quad n \rightarrow \infty, \\ E_n = \hbar\omega \left(n + \frac{1}{2}\right), \quad n = 0, 1, 2, \dots \quad (3)$$

Then, the function $W_n(x, p)$ corresponds to the classical trajectory in the phase space given by the coordinates x and p . Therefore, the delocalization of the Wigner distribution indicates quantum effects due to the uncertainty principle. The Wigner distribution provides information on quantum states by using the phase-space concept.

In the nucleon case, the Wigner distribution is defined for quarks by [12]

$$W_\Gamma(x, \vec{k}_\perp, \vec{r}) = \int \frac{d^3q}{(2\pi)^3} \langle \vec{q}/2 | \hat{w}_\Gamma(\vec{r}, k^+, \vec{k}_\perp) | -\vec{q}/2 \rangle, \\ \hat{w}_\Gamma(\vec{r}, k^+, \vec{k}_\perp) = \frac{1}{4\pi} \int d\xi^- d^2\xi_\perp e^{i(\xi^- k^+ - \vec{\xi}_\perp \cdot \vec{k}_\perp)} \\ \times \bar{\psi}(\vec{r} - \xi/2) \Gamma \psi(\vec{r} + \xi/2) \Big|_{\xi^+ = 0}. \quad (4)$$

Here, the x is the Bjorken scaling variable and it should not be confused with the space coordinate in Eqs. (1),

(2), and (3), ψ is the quark field, and Γ is a γ matrix which depends on the quark-distribution type. A gauge link needs to be introduced in Eq. (4) for satisfying the gauge invariance. The function $W_\Gamma(x, \vec{k}_\perp, \vec{r})$ provides a complete quantum mechanical description of the internal nucleon structure by supplying the phase space distribution at the longitudinal momentum fraction x , the transverse momentum \vec{k}_\perp , and the space position \vec{r} .

If this distribution is determined, it means a complete understanding on the quantum nature of the nucleon substructure from low to high energies. However, it is not realistic to determine the Wigner distribution experimentally because it contains six variables. Therefore, the distribution is integrated over some variables for practical measurements. Depending on the integral variables, we have following physics quantities:

$$\begin{aligned}
\int d^3r W_\Gamma(x, \vec{k}_\perp, \vec{r}) &\rightarrow \text{TMDs (uPDFs),} \\
\int d^2k_\perp W_\Gamma(x, \vec{k}_\perp, \vec{r}) &\rightarrow \text{GPDs,} \\
\int dx d^2k_\perp W_\Gamma(x, \vec{k}_\perp, \vec{r}) &\rightarrow \text{Form factors,} \\
\int d^3r d^2k_\perp W_\Gamma(x, \vec{k}_\perp, \vec{r}) &\rightarrow \text{PDFs.} \quad (5)
\end{aligned}$$

As obvious from these expressions, the TMDs and GPDs provide three-dimensional understanding of the nucleon by effectively including the PDFs and transverse distributions. Now, we introduce basic properties of the GPDs and also the GDAs which are the quantities obtained by the s and t channel crossing.

B. Generalized parton distributions

The GPDs have been investigated mainly for the nucleon in order to clarify the origin of the nucleon spin and the tomography, namely the determination of a three-dimensional view of the nucleon substructure. The GPDs can be measured in various reactions, virtual-Compton and meson-production processes in lepton scattering [13, 14] and also in lepton-pair [15] and meson production processes [16] at hadron beam facilities.

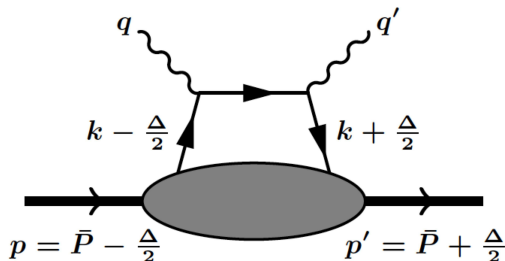


FIG. 1: Kinematics for GPDs.

The best process to probe the GPDs is the deeply virtual Compton scattering (DVCS) shown in Fig. 1. First, we define kinematical variables used for describing the DVCS and defining the GPDs [13, 18]. As shown in Fig. 1, p (q) and p' (q') are initial and final nucleon (photon) momenta, respectively. The initial photon is a virtual one, whereas the final photon is a real one. The average nucleon and photon momenta (\bar{P} and \bar{q}) and the momentum transfer Δ are defined by [19]

$$\bar{P} = \frac{p + p'}{2}, \quad \bar{q} = \frac{q + q'}{2}, \quad \Delta = p' - p = q - q'. \quad (6)$$

Then, the momentum-transfer-squared quantities are given by

$$Q^2 = -q^2, \quad \bar{Q}^2 = -\bar{q}^2, \quad t = \Delta^2. \quad (7)$$

From these quantities, we define the generalized scaling variable x and a skewness parameter ξ by

$$x = \frac{Q^2}{2p \cdot q}, \quad \xi = \frac{\bar{Q}^2}{2\bar{P} \cdot \bar{q}}. \quad (8)$$

The variable x indicates the lightcone momentum fraction carried by a quark in the nucleon. The skewness parameter ξ or the momentum Δ indicates the momentum transfer from the initial nucleon to the final one or the one between the quarks. Using these relations, we can express ξ in terms of x , t , and Q^2 as

$$\xi = \frac{x [1 + t/(2Q^2)]}{2 - x(1 - t/Q^2)} \simeq \frac{x}{2 - x} \quad \text{for } Q^2 \gg |t|. \quad (9)$$

Next, we express these quantities by lightcone variables. The lightcone coordinates a^\pm are defined by $a^\pm = (a^0 \pm a^3)/\sqrt{2}$, and \vec{a}_\perp is the transverse vector. Using these notations, we denote $a = (a^+, a^-, \vec{a}_\perp)$. Neglecting hadron masses, we express the hadron and photon momenta as

$$\begin{aligned}
p &\simeq (p^+, 0, \vec{0}_\perp), & p' &\simeq (p'^+, 0, \vec{0}_\perp), \\
q &\simeq \left(-xp^+, \frac{Q^2}{2xp^+}, \vec{0}_\perp\right), & q' &\simeq \left(0, \frac{Q^2}{2xp^+}, \vec{0}_\perp\right). \quad (10)
\end{aligned}$$

Here, the approximate equations are obtained due to the relation $(p^+)^2, Q^2 \gg M^2, |t|$. The momentum conservation indicates $p'^+ \simeq (1 - x)p^+$. Then, the skewness parameter ξ is expressed by the lightcone momenta as

$$-\frac{\Delta^+}{2P^+} = \frac{p^+ - p'^+}{p^+ + p'^+} = \frac{x}{2 - x} \simeq \xi \quad \text{for } Q^2 \gg |t|. \quad (11)$$

These variables x , ξ , and t are used for expressing the GPDs.

The GPDs for the nucleon are given by off-forward matrix elements of quark and gluon operators with a lightcone separation between nucleonic states [12, 13]. The

quark GPDs are defined by

$$\begin{aligned} & \int \frac{dy^-}{4\pi} e^{ix\bar{P}^+y^-} \langle p' | \bar{\psi}(-y/2)\gamma^+\psi(y/2) | p \rangle \Big|_{y^+=\bar{y}_\perp=0} \\ &= \frac{1}{2P^+} \bar{u}(p') \left[H_q(x, \xi, t)\gamma^+ + E_q(x, \xi, t) \frac{i\sigma^{+\alpha}\Delta_\alpha}{2M} \right] u(p). \end{aligned} \quad (12)$$

Here, $\sigma^{\alpha\beta}$ is defined by $\sigma^{\alpha\beta} = (i/2)[\gamma^\alpha, \gamma^\beta]$ and $\psi(y/2)$ is the quark field. The functions $H_q(x, \xi, t)$ and $E_q(x, \xi, t)$ are the unpolarized GPDs for the nucleon. The Dirac spinor for the nucleon is denoted as $u(p)$. There are also gluon GPDs $H_g(x, \xi, t)$ and $E_g(x, \xi, t)$ for the nucleon [13], but they are not used in this article for investigating internal structure of exotic-hadron candidates.

There are three important properties for the GPDs. First, the nucleonic GPDs $H(x, \xi, t)$ become usual PDFs for the nucleon in the forward limit ($\Delta, \xi, t \rightarrow 0$):

$$H_q(x, 0, 0) = q(x), \quad (13)$$

where $q(x)$ is an unpolarized parton distribution function (PDF) in the nucleon. Second, their first moments are the form factors of the nucleon:

$$\int_{-1}^1 dx H_q(x, \xi, t) = F_1(t), \quad \int_{-1}^1 dx E_q(x, \xi, t) = F_2(t), \quad (14)$$

where $F_1(t)$ and $F_2(t)$ are Dirac and Pauli form factors. Third, a second moment gives a quark orbital-angular-momentum contribution (L_q) to the nucleon spin:

$$\begin{aligned} J_q &= \frac{1}{2} \int dx x [H_q(x, \xi, t=0) + E_q(x, \xi, t=0)] \\ &= \frac{1}{2} \Delta q + L_q, \end{aligned} \quad (15)$$

where Δq is the quark-spin contribution and J_q is the total angular-momentum of quarks. This equation indicates that the nucleonic GPDs are important for clarifying the origin of the nucleon spin because quark and gluon spin contributions seem to be rather small for explaining the nucleon spin. From these properties in Eqs. (13) and (14), the GPDs contain both information on the longitudinal momentum distributions and transverse structure of the nucleon as the form factors. These facts indicate that the GPDs are valuable quantities for understanding basic properties of the nucleon from low to high energies. On the other hand, it is interesting to use these quantities for exotic-hadron studies because they have information on internal structure of hadrons.

C. Generalized distribution amplitudes

The GDAs are defined in the same manner with the GPDs in the s - t crossed channel as shown in Fig. 2. They describe the production of a hadron pair $h\bar{h}$ from a $q\bar{q}$ or gluon pair. First, we define kinematical variables

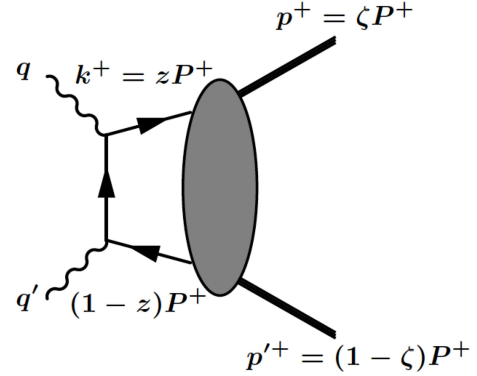


FIG. 2: Kinematics for GDAs. The process is a crossed channel to the GPD in Fig. 1.

for describing the $\gamma^*\gamma \rightarrow h\bar{h}$ process [13, 20, 21, 22]. The final hadron momenta are p and p' as shown in Fig. 2, P is their total momentum: $P = p + p'$ [19], and k is the quark momentum. The momenta q and q' are initial photon momenta. The photon with the momentum q is a virtual one with a typical scale larger than the QCD scale Λ , so that the factorization of the process into a soft part and a hard process should be valid [23]. Another photon with the momentum q' is considered to be a real one:

$$Q^2 = -q^2 \gg \Lambda^2, \quad q'^2 = 0. \quad (16)$$

The center-of-mass (c.m.) energy squared is s which is equal to the invariant-mass squared W^2 of the final hadron pair:

$$s = (q + q')^2 = (p + p')^2 = W^2. \quad (17)$$

The variables x_γ and ζ are defined by

$$x_\gamma = \frac{Q^2}{2q \cdot q'} = \frac{Q^2}{Q^2 + W^2}, \quad \zeta = \frac{p \cdot q'}{P \cdot q'}. \quad (18)$$

In the center of mass system of two final hadrons, the photon and hadron momenta are expressed as

$$\begin{aligned} q &= (q^0, 0, 0, |\vec{q}|), & q' &= (|\vec{q}|, 0, 0, -|\vec{q}|), \\ p &= (p^0, |\vec{p}| \sin \theta, 0, |\vec{p}| \cos \theta), \\ p' &= (p^0, -|\vec{p}| \sin \theta, 0, -|\vec{p}| \cos \theta), \end{aligned} \quad (19)$$

where θ is the scattering angle in the c.m. frame. Then, the variable ζ becomes

$$\zeta = \frac{p \cdot q'}{P \cdot q'} = \frac{p^+}{P^+} = \frac{1 + \beta \cos \theta}{2}, \quad (20)$$

where β is the velocity of a hadron

$$\beta = \frac{|\vec{p}|}{p^0} = \sqrt{1 - \frac{4m_h^2}{W^2}}, \quad (21)$$

Here, m_h is the mass of a final hadron h . Equation (20) indicates that the variable ζ is the lightcone momentum

ratio for a hadron in the hadron pair. Next, as for the lightcone momentum ratio for a quark in the hadron pair, we use the variable z which is given by

$$z = \frac{k \cdot q'}{P \cdot q'} = \frac{k^+}{P^+}, \quad (22)$$

The GDAs can be expressed in terms of these variables z , ζ , and s .

The GDAs are defined by the same lightcone operators as the GPDs between the vacuum and the hadron pair $h\bar{h}$ instead of initial and final hadron states for the GPDs [13]:

$$\Phi_q^{h\bar{h}}(z, \zeta, s) = \int \frac{dy^-}{2\pi} e^{i(2z-1)P^+y^-} \times \langle h(p) \bar{h}(p') | \bar{\psi}(-y/2) \gamma^+ \psi(y/2) | 0 \rangle \Big|_{y^+ = \bar{y}^+ = 0}, \quad (23)$$

which is a quark GDA. The gluon GDA is defined in the same way [13].

By considering the kinematical region of $Q^2 \gg W^2, \Lambda^2$, the process $\gamma^* \gamma \rightarrow h\bar{h}$ is factorized into two parts as shown in Fig. 2: a hard part described by photon interactions with quarks and a soft part given by the GDAs. In the same way, the $\gamma^* h \rightarrow \gamma h'$ is factorized at $Q^2 \gg -t, \Lambda^2$ into the hard part of quark interactions and the soft one given by the GPDs as shown in Fig. 1. Once the factorization can be applied for both processes, the GDAs are related to the GPDs by the s - t crossing. The $\gamma^* \gamma$ process $\gamma^* \gamma \rightarrow h\bar{h}$ at large Q^2 and $W^2 \ll Q^2$ should be related to the virtual Compton scattering on h ($\gamma^* h \rightarrow \gamma h$) at large Q^2 and $-t \ll Q^2$ by the s - t crossing. The crossing means to move the final state \bar{h} (p') to the initial h (p), which indicates that the momenta (p, p') of the GDAs should be replaced by ($p', -p$) in the GPDs. It corresponds to the variable changes [13, 21]:

$$z \leftrightarrow \frac{1-x/\xi}{2}, \quad \zeta \leftrightarrow \frac{1-1/\xi}{2}, \quad W^2 \leftrightarrow t. \quad (24)$$

These relations indicate that the GDAs are related to the GPDs by the relation:

$$\Phi_q^{h\bar{h}}(z, \zeta, W^2) \longleftrightarrow H_q^h \left(x = \frac{1-2z}{1-2\zeta}, \xi = \frac{1}{1-2\zeta}, t = W^2 \right). \quad (25)$$

Since there are more theoretical and experimental studies in the GPDs, this correspondence may seem to be convenient to estimate the GDAs for exotic hadrons by using an appropriate and simple function for the GPDs as explained in Sec. III A. However, we notice in Eq. (25) that the GDAs correspond to the GPDs in the *unphysical region* [24]. For example, the relation $1-2\zeta = 1/\xi$ with $|1-2\zeta| \leq 1$ indicates $|\xi| \geq 1$, which is an unphysical region of the GPDs. Furthermore, $x = (1-2z)/(1-2\zeta)$ suggests that x could be larger than one ($|x| \geq 1$) depending on z and ζ , and t is $t = s \geq 0$ although it satisfies

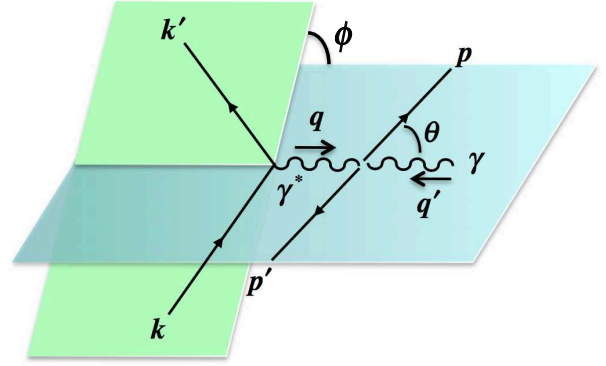


FIG. 3: (Color online) Kinematics of the $e + \gamma \rightarrow e + h\bar{h}$ process.

$t < 0$ in the spacelike reaction. These are also unphysical regions. Therefore, it is not straightforward how the GPDs could be used for the studies of GDAs. It is also noteworthy that Eq. (25) indicates the kinematical region $|\xi| \geq |x|$ which is specifically called as the Efremov-Radyushkin-Brodsky-Lepage (ERBL) region. Therefore, the correspondence of the GPDs and GDAs could be investigated by studying the kinematical region:

$$0 \leq |x| < \infty, \quad 0 \leq |\xi| < \infty, \quad |x| \leq |\xi|, \quad t \geq 0, \quad (26)$$

which is not necessarily the usual physical region of the GPDs. In any case, it is an interesting topic for future investigations on the correspondence between the GPDs and GDAs by considering the s - t crossing relation.

D. Cross section of $e + \gamma \rightarrow e + h\bar{h}$ and GDAs

Although the cross section of the two-photon process $\gamma^* \gamma \rightarrow h\bar{h}$ could be used for comparison with experimental data, we show the cross section of $e + \gamma \rightarrow e + h\bar{h}$ in this work. They are simply related by a kinematical factor, so either cross section can be shown theoretically for comparing them with experimental data [25] because we ignore the bremsstrahlung process as explained after Eq. (37). The bremsstrahlung process does not exist for neutral-meson pair productions.

The kinematics of this process is shown in Fig. 3. The initial and final electron momenta are denoted as k and k' , the virtual and real photon momenta are q and q' , respectively, and the final hadron momenta are p and p' . The scattering angle for the final hadron in the center of mass of the final hadrons is θ , and the scattering plane of the electron has the angle ϕ with respect to the reaction plane of $\gamma^* \gamma \rightarrow h\bar{h}$ as shown in the figure [21]. The cross

section for $e\gamma \rightarrow eh\bar{h}$ is given by

$$d\sigma = \frac{1}{4\sqrt{(k \cdot q')^2 - k^2 q'^2}} \bar{\sum}_{\lambda_\gamma, \lambda_e, \lambda'_e} |M(e\gamma \rightarrow e' h\bar{h})|^2 d\Phi_3,$$

$$d\Phi_3 = \frac{d^3 p}{2E_h(2\pi)^3} \frac{d^3 p'}{2E'_h(2\pi)^3} \frac{d^3 k'}{2E'_e(2\pi)^3} \times (2\pi)^4 \delta^4(k + q' - p - p' - k'), \quad (27)$$

where $d\Phi_3$ is the three-body phase space factor, and the summation indicates the spin averages. The center-of-mass-energy square is given by

$$s_{e\gamma} = (k + q')^2 = 2k \cdot q', \quad (28)$$

by neglecting the electron mass.

The matrix element for $e\gamma \rightarrow e'h\bar{h}$ is given by

$$iM(e\gamma \rightarrow e'h\bar{h}) = \bar{u}(k') (-ie\gamma_\mu) u(k) \times \frac{-ig^{\mu\nu}}{q^2} (-iT_{\nu\rho}) \varepsilon^\rho(q'), \quad (29)$$

where $\varepsilon^\rho(q')$ is the polarization vector of the real photon. The polarization vectors of the photons are given by

$$\varepsilon_\mu^{(\pm)}(q) = \frac{1}{\sqrt{2}} (0, \mp 1, -i, 0), \quad \varepsilon_\mu^{(0)}(q) = \frac{1}{\sqrt{2}} (|\vec{q}|, 0, 0, q^0),$$

$$\varepsilon_\mu^{(\pm)}(q') = \frac{1}{\sqrt{2}} (0, \mp 1, +i, 0). \quad (30)$$

The hadron tensor for $\gamma^*\gamma \rightarrow h\bar{h}$ is defined by

$$T_{\mu\nu} = i \int d^4\xi e^{-i\xi \cdot q} \langle h(p) \bar{h}(p') | T J_\mu^{em}(\xi) J_\nu^{em}(0) | 0 \rangle. \quad (31)$$

Considering a reaction process with the condition $Q^2 \gg \Lambda^2$, we factorize it into a hard part with the photon interactions to produce a $q\bar{q}$ pair and a soft part for producing a $h\bar{h}$ pair from the $q\bar{q}$ pair as shown in Fig. 2. Namely, it is expressed by the summation of the quark GDAs $\Phi_q^{h\bar{h}}$ in the leading order of α_s by neglecting gluon GDAs as [21]

$$T_{\mu\nu} = -g_{T\mu\nu} e^2 \sum_q \frac{e_q^2}{2} \int_0^1 dz \frac{2z-1}{z(1-z)} \Phi_q^{h\bar{h}}(z, \zeta, W^2),$$

$$\Phi_q^{h\bar{h}}(z, \zeta, W^2) = \int \frac{dx^-}{2\pi} e^{-izP^+x^-} \times \langle h(p) \bar{h}(p') | \bar{q}(x^-) \gamma^+ q(0) | 0 \rangle_{x^+=0, \vec{x}_\perp=0}, \quad (32)$$

where $g_{T\mu\nu}$ is defined by

$$g_{T\mu\nu} = -1 \quad \text{for } \mu = \nu = 1, 2, \\ = 0 \quad \text{for } \mu, \nu = \text{others}. \quad (33)$$

Equation (32) is the leading-twist expression which is valid at $Q^2 \gg \Lambda^2$, and higher-twist and higher-order terms are neglected.

We define helicity amplitudes by

$$A_{ij} = \frac{1}{e^2} \varepsilon_\mu^{(i)}(q) \varepsilon_\nu^{(j)}(q') T^{\mu\nu}, \\ i = -, 0, +, \quad j = -, +. \quad (34)$$

Using the relation $\varepsilon_\mu^{(+)}(q) \varepsilon_\nu^{(+)}(q') g_T^{\mu\nu} = -1$, we obtain, for example, A_{++} as

$$A_{++} = \sum_q \frac{e_q^2}{2} \int_0^1 dz \frac{2z-1}{z(1-z)} \Phi_q^{h\bar{h}}(z, \zeta, W^2), \quad (35)$$

and another one A_{--} is also the same, $A_{--} = A_{++}$. In this way, the matrix element part of the cross section becomes

$$\bar{\sum}_{\lambda_\gamma, \lambda_e, \lambda'_e} |M|^2 = \frac{64\pi^3 \alpha^3}{Q^2(1-\varepsilon)} |A_{++}|^2. \quad (36)$$

Here, the ε is the ratio of longitudinal and transverse fluxes of the virtual photon, and a virtual-photon cross section is generally written as $\sigma \propto (\sigma_T + \varepsilon\sigma_L)$ by the transverse and longitudinal cross sections σ_T and σ_L , respectively [26]. The ε is expressed by another variable y as

$$\varepsilon = \frac{1-y}{1-y+y^2/2}, \quad y \equiv \frac{q \cdot q'}{k \cdot q'} = \frac{Q^2 + W^2}{s_{e\gamma}}. \quad (37)$$

In principle, other helicity amplitudes such as A_{-+} and A_{0+} should contribute to the matrix element in Eq. (36). However, the leading-twist and leading-order expression is introduced in Eq. (32), so that it is expressed consequently only by the amplitude A_{++} . As explained in Ref. [21], relative contributions of $\gamma^*\gamma$ and bremsstrahlung processes are given by $1/(Q^2(1-\varepsilon))$ and $2\beta^2/(W^2\varepsilon)$, respectively. The bremsstrahlung part is small in our kinematics of Sec. III, so that it is neglected. Next, we calculate the phase space factor in Eq. (27) by using the polar and azimuthal angles θ and ϕ in the the c.m. frame of $h\bar{h}$ as defined in Eq. (19) and Fig. 3. It is obtained as

$$d\Phi_3 = \frac{\beta}{8 \cdot 64\pi^4 s_{e\gamma}} dQ^2 dW^2 d(\cos\theta) d\phi. \quad (38)$$

Substituting Eqs. (36) and (38) into Eq. (27), we finally obtain the cross section

$$\frac{d\sigma}{dQ^2 dW^2 d\cos\theta} = \frac{\beta \alpha^3}{8s_{e\gamma}^2 Q^2(1-\varepsilon)} |A_{++}(\zeta, W^2)|^2, \quad (39)$$

where the cross section is integrated over ϕ . The variable ζ and the angle θ are related by Eq. (20), and β is given in Eq. (21). We should note that the cross section generally depends on the angle ϕ [21]. However, the higher-twist terms in the cross sections are dropped in Eq. (39), which originally comes from the leading-twist expression of Eq. (32). It leads to the cross section, which is independent of the azimuthal angle ϕ . The purpose of this work is to investigate basic signatures of exotic hadrons in the two-photon processes by neglecting small perturbative QCD corrections. In future, the higher-twist corrections could become necessary for the detailed comparison between theory and experimental data.

III. RESULTS

A. Generalized parton distributions of exotic hadrons

For numerical analysis of cross sections with GPDs and GDAs, realistic functions are needed for these distributions. A full theoretical information is not yet available for these distributions. However, there are some theoretical studies on the appropriate parametrization for the GPDs although they are scarce for the GDAs.

Because the longitudinal part of the GPDs indicates the longitudinal momentum distributions of partons and the transverse part is related to the two-dimensional form factors, the simplest idea is to assume a GPD as the corresponding PDF multiplied by a form factor. However, it is too simple to describe the realistic hadron. The large- x distribution is related to a hard valence-quark with large momentum and it should be confined in a small space region, namely the transverse distribution is also confined in a small region. On the other hand, small- x partons are rather loosely distributed in a larger space. Namely, the two-dimensional form factors are different in small- and large- x regions. The simple multiplication of the form factor and the PDF cannot reflect this nature. In Ref. [27], the mixed functional form is proposed for the nucleon by assuming a Gaussian distribution for the transverse part to improve such an issue.

We may use this kind of idea for exotic hadron studies by supplying the longitudinal momentum distribution $f_n(x)$ of an exotic hadron with n valence quarks and the transverse form factor $F_n^h(t, x)$:

$$H_q^h(x, \xi = 0, t) = f_n(x) F_n^h(t, x), \quad (40)$$

for valence quarks. However, the ERBL region $|\xi| > x$ cannot be described by this functional form because the process is related to a meson distribution amplitude. A more sophisticated function type is used in Ref. [28] by including the ERBL region. Since this article is a first step toward GPDs and GDAs of exotic hadrons, we simply considered the simple case of Eq. (40) in the following discussions. Significant efforts are still needed for realistic tomography of exotic hadrons by using the GPDs and GDAs.

B. Parton distribution functions of exotic hadrons

The longitudinal momentum distributions of partons have been investigated extensively by various processes including charged-lepton and neutrino deep inelastic scattering (DIS), Drell-Yan processes, and W , Z , jet, and hadron productions. Now, the details of the PDFs are accurately determined except for extreme kinematical conditions. The parton distributions in the pion have been determined by Drell-Yan processes. Since the unstable pion cannot be used as a fixed target, there is no deep in-

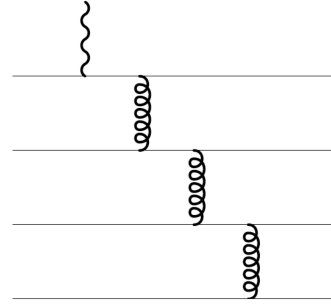


FIG. 4: Constituent-counting rule for a tetra-quark hadron. A three-gluon-exchange process is shown for a typical exclusive process. There are many other processes depending how the gluon lines are attached to the quarks.

elastic measurement. The exotic hadron candidates cannot be used either as a fixed target or a beam for the Drell-Yan. Therefore, the longitudinal momentum distribution cannot be measured by these usual methods. However, let us consider a *gedankenexperiment* by which the PDFs or the GPDs of the exotic hadrons can be obtained by assuming a stable target.

We explain our guideline for the PDFs of the exotic hadrons if they were measured. We consider only the valence-quark distributions. Including PDFs in exotic hadrons, we denote the sum of valence-quark distributions as $f_n(x)$, where n is the number of valence quarks in a hadron, by taking a suitable low Q^2 scale ($Q^2 = 1 \sim$ a few GeV^2) for the first estimate. In future, scaling violation may be considered; however, it is not the stage to investigate such details of Q^2 dependence because there is the first work on possible PDFs of exotic hadrons.

If the nucleon consists of three valence quarks and if the nucleon momentum is equally shared by the quark momenta, the distribution has a peak at $x = 1/3$: $f_3(x) \sim \delta(x - 1/3)$. However, the quarks interact with each other by exchanging gluons, so that their momenta are redistributed. The distribution should vanish at $x = 1$ kinematically, and the x dependence at $x \rightarrow 1$ is theoretically described by the constituent-counting rule, obtained by hard gluon exchanges between quarks for exclusive processes as shown in Fig. 4 for a tetra-quark hadron. It leads to the x dependence $(1 - x)^\beta$ at $x \rightarrow 1$. Including a polynomial form of x^α , which is motivated, for example, by the Regge theory [26], at smaller x , we have a simple functional form of the parton distributions as

$$f_n(x) = C_n x^{\alpha_n} (1 - x)^{\beta_n}, \quad (41)$$

for hadrons including exotic ones.

The three constants C_n , α_n , and β_n are constrained by the valence-quark number n and the momentum $\langle x \rangle_q$ carried by the valence quarks:

$$\int_0^1 dx f_n(x) = n, \quad \int_0^1 dx x f_n(x) = \langle x \rangle_q. \quad (42)$$

Using the constant β_n and the number of constituents n , we have C_n and α_n as

$$C_n = \frac{\langle x \rangle_q}{B(\alpha_n + 2, \beta_n + 1)}, \quad \alpha_n = \frac{\langle x \rangle_q (\beta_n + 2) - n}{n - \langle x \rangle_q}. \quad (43)$$

The large- x limit ($x \rightarrow 1$) corresponds to the exclusive process shown in Fig. 4. There exists the Drell-Yan-West relation between the Dirac form factor at large Q^2 and the structure function F_2 at $x \rightarrow 1$ [29, 30]. It indicates $F_2(x) \sim (1-x)^{2\gamma-1}$ at $x \rightarrow 1$ for the form-factor function $F_1(Q^2) \sim 1/(Q^2)^\gamma$ at large Q^2 . This relation was derived before the advent of QCD; however, the constituent-counting rule was derived in perturbative QCD by describing the process by hard gluon exchanges typically shown in Fig. 4 [31]. As explained in Ref. [10], the large momentum provided by the hard photon should be shared by four quark constituents by exchanging three hard gluons so that the initial and final states are the same. From the hard gluon and quark propagators together with other kinematical factors, the process indicates that the factor γ expressed by the number of active constituents n as $\gamma = n-1$ in the form factor at large Q^2 . It leads to the overall factor of $(1-x)^{\beta_n}$, $\beta_n = 2n-3$ [29] with the number of valence quarks n . Because of this number counting, it is called the constituent-counting rule for structure functions at $x \rightarrow 1$ and also for the form factors. However, it was pointed out that there is an additional spin factor $\Delta S_z = |S_z^q - S_z^h|$ due to the helicity conservation [32], so that the factor becomes $\beta_n = 2n - 3 + 2\Delta S_z$. It does not matter for the spin-1/2 nucleon because $\Delta S_z = 0$; however, it affects the pion because of $\Delta S_z = 1/2$. In discussing a spin-1/2 penta-quark hadron candidate such as $\Lambda(1405)$, it also does not matter for the unpolarized distributions. For showing the distribution for a tetra-quark hadron, we assume that it is spin-0 particle so as to have the factor $\Delta S_z = 1/2$ by considering, for example, $f_0(980)$ and $a_0(980)$.

Using Eqs. (41) and (43), we calculate the PDFs for hadrons with the valence-quark number $n = 2, 3, 4$, or 5, namely for ordinary $q\bar{q}$ -type mesons, qqq type baryons, tetra-quark and penta-quark hadrons. Their valence-quark distributions are shown by the solid and dashed curves in Fig. 5. The average momentum fraction $\langle x \rangle_q$ is considered to be in the range $0.4 \sim 0.5$, so that it is taken as $\langle x \rangle_q = 0.47$ in the figure. The distributions have peaks at about $x = 1/n$. For example, there are two valence quarks in the pion, so that it has a wide- x distribution with the peak position at $x \sim 1/2$. As the valence-quark number becomes larger for tetra-quark and penta-quark hadrons, the hadron momentum is shared by more (four or five) valence quarks, so that the distributions become softer as the peak moves to smaller- x locations.

First, we need to confirm that the simple counting-rule estimates are reasonable in comparison with experimental data. There exist experimental measurements for the PDFs in the pion and the proton. The pionic PDFs are determined by the Drell-Yan, and the proton PDFs are by various measurements including leptonic

DIS. Because the optimum PDFs are determined from global analyses of many experimental measurements and the PDFs cannot be directly measured, the experimental data cannot be plotted in the figure. Therefore, the typical parametrizations obtained by the global analyses are shown in Fig. 5.

Since the counting-rule PDFs do not contain a specific Q^2 scale, there is uncertainty how to choose Q^2 in such parametrizations. We chose $Q^2=2 \text{ GeV}^2$ in Fig. 5 as a typical Q^2 which is close to the hadronic scale and yet it is the region where the perturbative QCD can be applied. The valence-quark distributions have strong constraints by the sum rules coming from hadron charges and baryon numbers. Therefore, the distribution shapes do not change drastically depending on Q^2 due to the sum-rule constraints in addition to the fact that the PDFs have, in general, weak Q^2 dependence in the logarithmic Q^2 form [33].

The PDFs at $Q^2=2 \text{ GeV}^2$ are taken from the next-to-leading order (NLO) distributions of the fit-3 in Ref. [34] for the pion and in Ref. [35] for the proton. Although the comparison of the results in Fig. 5 depends on the choice of $\langle x \rangle_q = 0.47$ and the Q^2 value, the counting-rule PDFs are reasonably consistent with the current experimental measurements for the pion and proton PDFs, although the detailed x dependence of the pion functions with $\beta_\pi = 1$ and 2 is slightly different from the experimental determination shown by the dotted curve. Therefore, we believe that the valence-quark distributions for the tetra-quark and penta-quark hadrons in Fig. 5 should be reasonable.

We found that the longitudinal momentum distribution of the valence quarks has a characteristic feature that

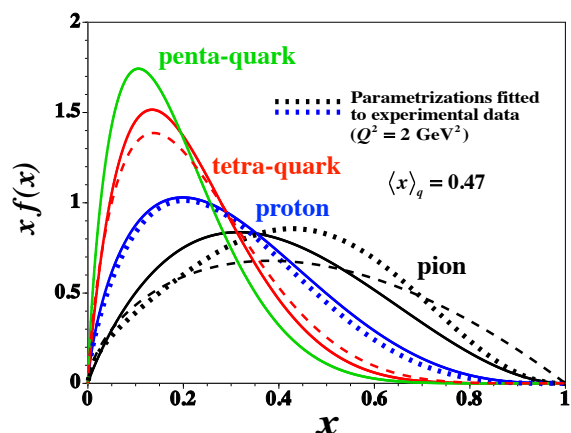


FIG. 5: (Color online) PDFs of exotic hadrons in comparison with parametrizations of pion and proton PDFs. The solid curves are calculated by Eqs. (41) and (43) with $\beta_n = 2n - 3 + 2\Delta S_z$ [32]. The spin factor is $\Delta S_z = 0$ for the proton and penta-quark, whereas it is $\Delta S_z = 1/2$ for the pion and tetra-quark. In comparison, the native estimates with $\beta_n = 2n - 3$ [29] are shown by the dashed curves. The dotted curves indicate the PDF parametrizations at $Q^2=2 \text{ GeV}^2$ for the proton and pion.

the distribution is shifted toward the smaller- x region. If such a signature is found experimentally, it should be a key discovery in exotic hadron search because a clear signature is difficult to be found in low-energy measurements of hadron masses and decays. However, the exotic hadron candidates cannot be used for fixed targets and beams, so that possible methods should be studied by including transition GPDs [14, 16]. In this article, we propose that the GPDs and GDAs (and also TMDs) are appropriate quantities to be investigated because the exotic hadrons could exist in the final state, rather than the initial targets and beams, and because the GPDs and GDAs contain the PDFs in their functions as the longitudinal-momentum dependence.

C. Transverse form factors of exotic hadrons

Next, we show typical transverse form factors $F_n^h(t, x)$, which is given in Eq. (40). A simple form of this function is given in as an exponential form [27]:

$$F_n^h(t, x) = e^{(1-x)t/(x\Lambda^2)}, \quad (44)$$

where Λ is cutoff parameter for the transverse momentum. The transverse density is given by its Fourier transform

$$\begin{aligned} \rho(r_\perp, x) &= \int \frac{d^2q_\perp}{(2\pi)^2} e^{-i\vec{q}_\perp \cdot \vec{r}_\perp} F_n^h(t = -q_\perp^2, x) \\ &= \frac{x\Lambda^2}{4\pi(1-x)} e^{-x\Lambda^2 r_\perp^2 / (4(1-x))}, \end{aligned} \quad (45)$$

and the root-mean-square (rms) radius is then expressed by the cutoff parameter as

$$\langle r_\perp^2 \rangle = \frac{4(1-x)}{x\Lambda^2}. \quad (46)$$

As for the pion and nucleon form factors, monopole and dipole forms ($1/(|t| + \Lambda^2)$, $1/(|t| + \Lambda^2)^2$) are usually used, so that the Gaussian form could be too steep as a function of q_\perp^2 . The dipole form factor for the nucleon corresponds to the exponential density distribution, and the Gaussian form factor does to the Gaussian as shown in Eq. (45). In nuclear physics, such a Gaussian form factor is realistic on light nuclei such as ${}^6\text{Li}$ [36]. In any case, the functional form depends on an exotic hadron type and it should be the topic of future investigations, and we do not step into such details in this work.

As an example, the transverse form factor is shown as a function of q_\perp^2 in Fig. 6. The form factors for the cutoff parameters, $\Lambda=0.5$ and 1.0 GeV, are shown at $x=0.2$ and 0.4 . The rms radii are $\sqrt{\langle r_\perp^2 \rangle} = 0.48, 0.79, 0.97,$ and 1.58 fm for the variable x and the cutoff parameter Λ , $(x, \Lambda(\text{GeV})) = (0.4, 1.0), (0.2, 1.0), (0.4, 0.5), (0.2, 0.5)$, respectively. The three-dimensional charge radii are measured as 0.877 fm for the proton and 0.672 fm for π^\pm [37]. Because the current transverse radius depends on the longitudinal momentum fraction x , the transverse radius is

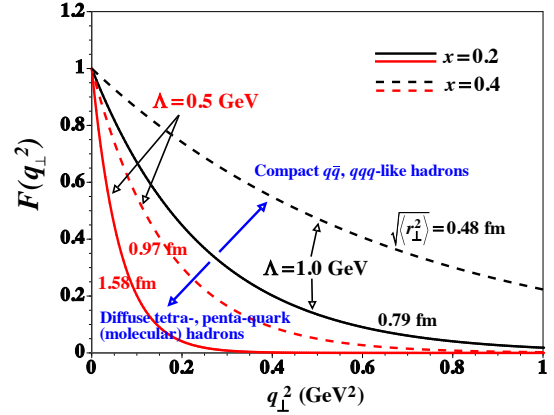


FIG. 6: (Color online) Transverse form factors for $x = 0.2, 0.4$ and $\Lambda = 0.5, 1.0$ GeV. The r.m.s radius is $\sqrt{\langle r_\perp^2 \rangle} = 0.48, 0.79, 0.97,$ and 1.58 fm for $(x, \Lambda(\text{GeV})) = (0.4, 1.0), (0.2, 1.0), (0.4, 0.5), (0.2, 0.5)$, respectively.

not equal to the rms radius. However, the middle region of the four curves corresponds to the “ordinary” hadrons of the $q\bar{q}$ and qqq types. On the other hand, the tetra- and penta-quark hadrons, particularly the molecular type hadrons, have large spacial distributions, so that the momentum distribution becomes softer as typically indicated by the curves with $\Lambda=0.5$ GeV.

Summary of exotic signatures in the GPDs

The simple GPD parametrization of Eq. (40) indicates that internal configurations of exotic hadrons could be clarified by finding typical exotic signatures in the longitudinal and transverse distributions.

- (1) Softening of longitudinal momentum distribution: As indicated in Fig. 5, the longitudinal momentum distribution, namely the PDF, should shift to smaller x as it becomes tetra- or penta-quark hadrons as expected from the quark counting rule and the momentum fraction carried by quarks.
- (2) Softening of transverse form factor: The transverse momentum distribution becomes softer for tetra- and penta-quark hadrons, especially for molecular-type hadrons, than the one expected from ordinary compact $q\bar{q}$ or qqq type hadrons.

However, exotic hadrons are unstable particles and they cannot be used as a target in experimental measurements. A possible solution is to investigate a production process of an exotic hadron, which is associated with transition GPDs [14, 16] from an ordinary hadron such as the proton to an exotic one. An exclusive lepton-pair production process $\pi + N \rightarrow \mu^+ \mu^- + N$ can be used for investigating the nucleonic GPDs [15]. The exclusive $\mu^+ \mu^-$ production could be valuable also for investigating exotic hadrons such as $\Lambda(1405)$ by the form of transition GPDs from the proton to $\Lambda(1405)$ as illustrated in Fig. 7. Since high-momentum beams of protons and pions, possibly also kaons in future, will become available at J-PARC, an experimental proposal is considered

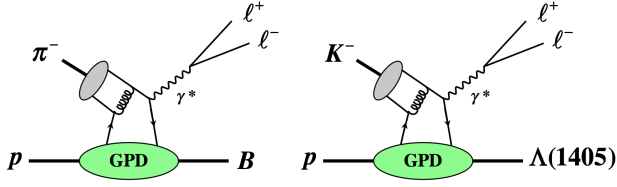


FIG. 7: (Color online) Examples of transition GPDs by exclusive dimuon production processes with pion and kaon beams. $\Lambda(1405)$ is an exotic hadron candidate.

[38]. We expect to investigate such a topic as our future work. Here, we discuss an alternative method by using the GDAs, which the exotic hadrons are studied by time-like production processes.

D. Internal structure of exotic hadrons by GDAs in electron-positron annihilation

In order to estimate the cross section for $e\gamma \rightarrow e'h\bar{h}$ by Eqs. (35) and (39), the actual functions of GDAs need to be introduced. There was a work on the GDAs on their impact-parameter dependence [39]. In our studies, we use a simple function, which satisfies the sum rules for the quark GDAs for the isospin $I = 0$ two-meson final states [21, 40]:

$$\int_0^1 dz \Phi_q^{h\bar{h}(I=0)}(z, \zeta, W^2) = 0, \\ \int_0^1 dz (2z-1) \Phi_q^{h\bar{h}(I=0)}(z, \zeta, W^2) \\ = -2M_{2(q)}^h \zeta(1-\zeta) F_{h(q)}(W^2), \quad (47)$$

where $M_{2(q)}^h$ is the momentum fraction carried by quarks, and $F_{h(q)}(W^2)$ is a form factor of the quark part of the energy-momentum tensor [41]. One may note that the kinematical condition $Q^2 \gg W^2$ is needed for the factorization of Fig. 2. If it is satisfied, the two-meson final state originates from the $q\bar{q}$ state from $\gamma^*\gamma$, so that only the $I = 0$ state is allowed. A simple functional form to satisfy these conditions is

$$\Phi_q^{h\bar{h}(I=0)}(z, \zeta, W^2) \\ = N_{h(q)} z^\alpha (1-z)^\beta (2z-1) \zeta(1-\zeta) F_{h(q)}(W^2), \quad (48)$$

where the normalization constant is given by

$$N_{h(q)} = -\frac{2M_{2(q)}^h}{B(\alpha+1, \beta+1)} \\ \times \frac{(\alpha+\beta+2)(\alpha+\beta+3)}{(\alpha+1)(\alpha+2) + (\beta+1)(\beta+2) - 2(\alpha+1)(\beta+1)}. \quad (49)$$

In Eq. (48), a flavor-independent functional form is used except for the normalization factor.

First, as the x -dependent PDFs indicated exotic signature in Fig. 5, the z -dependent function should reflect some exotic features because the variables x and z are

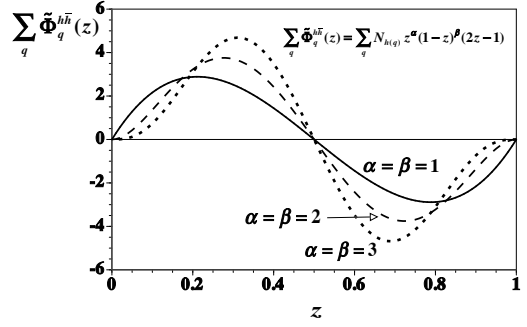


FIG. 8: z dependence is shown for the GDA $\tilde{\Phi}_q^{h\bar{h}}(z) = N_{h(q)} z^\alpha (1-z)^\beta (2z-1)$ by taking $\alpha = \beta = 1, 2,$ and 3 . They are shown by the solid, dashed, and dotted curves, respectively.

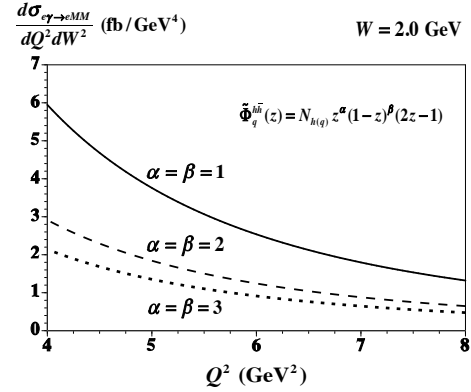


FIG. 9: Effect on the cross section $d\sigma/(dQ^2 dW^2)$ at $W = 2$ GeV from the z dependence in the GDA $\tilde{\Phi}_q^{h\bar{h}}(z) = N_{h(q)} z^\alpha (1-z)^\beta (2z-1)$ with $\alpha = \beta = 1, 2,$ and 3 . They are shown by the solid, dashed, and dotted curves, respectively. Here, the hadron h is f_0 or a_0 , and $n = 2$ is taken in the form factor of Eq. (50).

related by Eq. (24). However, we could not find a useful relation like the counting rule at $x \rightarrow 1$ in the PDFs for restricting the functional form. Because small x corresponds to $z \rightarrow 1/2$, the functional variation for exotic hadrons could correspond to the variation of the constants α and β . Therefore, we took $\alpha = \beta = 1, 2,$ and 3 to show its variation. The results are shown for the z dependent part $\sum_q \tilde{\Phi}_q^{h\bar{h}(I=0)}(z) = \sum_q N_{h(q)} z^\alpha (1-z)^\beta (2z-1)$ in Fig. 8 by taking $\sum_q M_{2(q)}^h = 0.5$. Then, their effects on the cross section are shown in Fig. 9. The form factor of Eq. (50) is used with $n = 2$. As the function $\sum_q \tilde{\Phi}_q^{h\bar{h}(I=0)}(z)$ becomes steep as shown in Fig. 8 with increasing α and β , the cross section becomes smaller. In order to clarify the z -dependent function, we need an estimate of the GDAs based on a theoretical model.

As for the form factor of the energy-momentum tensor, we employ a simple form suggested by the constituent-counting rule in perturbative QCD [42]:

$$F_{h(q)}(W^2) = \frac{1}{[1 + (W^2 - 4m_h^2)/\Lambda^2]^{n-1}}, \quad (50)$$

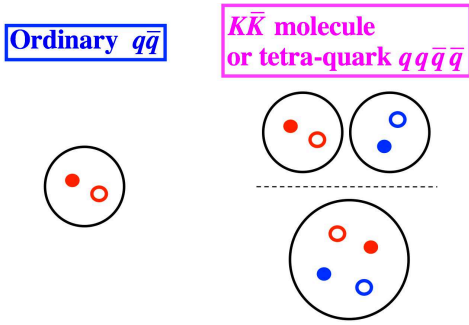


FIG. 10: (Color online) Schematic picture of f_0 and a_0 mesons, which are exotic-hadron candidates. It is likely that they are $K\bar{K}$ molecule or tetra-quark hadron. Because their sizes and internal constituents are different from the ordinary $q\bar{q}$ -type mesons, they should be distinguished by the hadron tomography by using the GDAs.

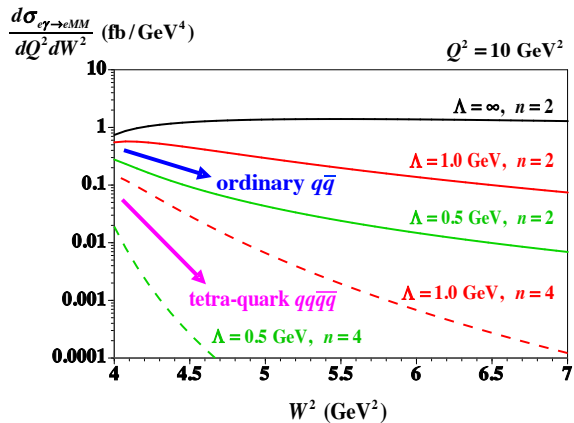


FIG. 11: (Color online) Form-factor effects are shown on the cross section $d\sigma/(dQ^2 dW^2)$ as a function of the invariant mass squared W^2 at $Q^2 = 10$ GeV. The number of constituents is taken as $n = 2$ or 4 , and the cutoff parameter is $\Lambda = \infty, 1.0, 0.5$ GeV, and we take $\alpha = \beta = 1$. Here, the hadron h is f_0 or a_0 . Considering the hadron size and the number of constituents, we expect that the slope of W^2 is much larger if the hadron has an exotic tetra-quark ($qq\bar{q}\bar{q}$) configuration.

where Λ is the cutoff parameter, which indicates the hadron size, n is the number of active constituents, and it is normalized as $F_{h(q)}(4m_h^2) = 1$. Here, the phase factor does not exist because the bremsstrahlung process is neglected. It is $n = 2$ for an ordinary $q\bar{q}$ hadron, whereas $n = 4$ for a $K\bar{K}$ molecule or a tetra-quark hadron as illustrated in Fig. 10.

Using the form factor together with the GDA expression in Eq. (48), we obtain the cross section for $e + \gamma \rightarrow e + h + \bar{h}$ as the function of W^2 in Fig. 11. If the a_0 and f_0 are ordinary hadrons consist of u and d quarks ($u\bar{d}$, $(u\bar{u} \pm d\bar{d})/\sqrt{2}$, $d\bar{u}$), the summation over the valence quarks becomes $\sum_q e_q^2 M_{2(q)}^h = (5/18) \sum_a M_{2(q)}^h$ by assuming that $M_{2(q)}^h$ is flavor independent, whereas the factor is $\sum_q e_q^2 M_{2(q)}^h = (1/9) \sum_a M_{2(q)}^h$ if the f_0 is $s\bar{s}$. If the a_0 and f_0 are tetra-quark hadrons ($u\bar{s}s\bar{d}$, $(u\bar{u} \pm d\bar{d})s\bar{s}/\sqrt{2}$,

$s\bar{u}d\bar{s}$), the factor is $\sum_q e_q^2 M_{2(q)}^h = (7/18) \sum_a M_{2(q)}^h$. We took into account these factors; however, the $s\bar{s}$ configuration is not shown in the figure. The cross sections for $s\bar{s}$ should be obtained simply by the $n = 2$ cross sections multiplied by $(2/5)^2$. The Q^2 value should be large enough so that the factorization into the hard part and the GDAs is satisfied. However, if it too large, the cross section becomes too small to be measured by the current Belle and BaBar experiments. As a compromise of these conflicting conditions, $Q^2 = 10$ GeV² is taken in the figure. The number of constituent for f_0 and a_0 is taken as $n = 2$ or 4 in the form factor by considering the ordinary $q\bar{q}$ or tetra-quark ($qq\bar{q}\bar{q}$) state. The cutoff parameter is taken as $\Lambda = \infty, 1.0, 0.5$ GeV. The cutoff $\Lambda = 1.0$ GeV roughly corresponds to the proton size, and 0.5 GeV is for a more diffuse state. Just for a typical illustration, we show expected tendency by the cutoff and the constituent number n if the hadron h is $q\bar{q}$ or $qq\bar{q}\bar{q}$. There are five curves and their W^2 slopes are distinctly different, so that the internal configuration of f_0 and a_0 should be determined by the cross-section measurements by the Belle and BaBar experiments. If a high-energy linear collider is realized in future, it has an advantage that larger W^2 and Q^2 regions should be probed to clarify the W^2 slope. In any case, the slope data in the region $W^2 = 4-6$ GeV² regions should be obtained by the current Belle and BaBar. In this way, the internal structure of exotic hadrons, for example f_0 and a_0 , should be clarified by the hadron tomography technique, especially by using the GDAs.

IV. SUMMARY

It is difficult to find a clear signature of exotic hadrons from usual low-energy measurements such as masses, spins, parities, and decay widths. Since the appropriate degrees of freedom are quarks and gluons at high energies, it is appropriate to use high-energy hadron reactions, especially by GPDs and GDAs. In this work, we showed exotic signatures in the GPDs as the longitudinal momentum distributions and transverse form factors. We also explained similar exotic signatures in the GDAs by the functional form of z and the energy-momentum form factor. Then, we showed their exotic effects on the cross section of $e + \gamma \rightarrow e + h + \bar{h}$. In particular, we found that there is a distinct signature of exotic nature in the slope of the invariant-mass squared W^2 .

The tomography of exotic hadrons is a new promising approach of exotic hadron studies for clarifying the internal structure of exotic hadrons by using the currently developing field of GPDs and GDAs.

Acknowledgments

The authors thank M. Diehl, V. Guzey, and A. Radyushkin for communications on GPD parametrization and S. Uehara for discussions on exotic-hadron studies at Belle. They also thank W.-C. Chang, J.-C. Peng, and S. Sawada for communications on J-PARC measure-

-
- [1] R. L. Jaffe, Phys. Rept. **409**, 1 (2005).
- [2] For example, see J. Brodzicka *et al.*, Prog. Theor. Exp. Phys. **2012**, 04D001 (2012).
- [3] J. Beringer *et al.* (Particle Data Group), Phys. Rev. D **86**, 010001 (2012).
- [4] F. E. Close and N. A. Törnqvist, J. Phys. G **28**, R249 (2002); C. Amsler and N. A. Törnqvist, Phys. Rept. **389**, 61 (2004).
- [5] R. L. Jaffe, Phys. Rev. D **15**, 267 & 281 (1977); J. D. Weinstein and N. Isgur, Phys. Rev. Lett. **48** (1982) 659; D. Black, A. H. Fariborz, and J. Schechter, Phys. Rev. D **61**, 074001 (2000); G. 't Hooft, G. Isidori, L. Maiani, A. D. Polosa, V. Riquer, Phys. Lett. B **662**, 424 (2008).
- [6] S. Kumano and V. R. Pandharipande, Phys. Rev. D **38**, 146 (1988); F. E. Close, N. Isgur, and S. Kumano, Nucl. Phys. B **389**, 513 (1993).
- [7] T. Sekihara and S. Kumano, arXiv:1311.4637 and references therein.
- [8] M. Hirai, S. Kumano, M. Oka, and K. Sudoh, Phys. Rev. D **77** (2008), 017504.
- [9] R. Seidl, personal communications on KEK-B experiments (2012).
- [10] H. Kawamura, S. Kumano, and T. Sekihara, Phys. Rev. D **88**, 034010 (2013).
- [11] M. Diehl, B. Pire, and L. Szymanowski, Phys. Lett. B **584**, 58 (2004); I. V. Anikin, B. Pire, L. Szymanowski, O. V. Teryaev, and S. Wallon, Phys. Rev. D **70**, 011501(R) (2004); **71**, 034021 (2005)
- [12] K. Goetze, M. V. Polyakov, and M. Vanderhaeghen, Prog. Part. Nucl. Phys. **47**, 401 (2001); X.-D. Ji, Ann. Rev. Nucl. Part. Sci. **54**, 413 (2004); A. V. Belitsky and A. V. Radyushkin, Phys. Rept. **418**, 1 (2005).
- [13] M. Diehl, Phys. Rept. **388**, 41 (2003); M. Diehl and P. Kroll, Eur. Phys. J. C **73** (2013) 2397.
- [14] L. L. Frankfurt, M. V. Polyakov, M. Strikman, and M. Vanderhaeghen, Phys. Rev. Lett. **84**, 2589 (2000).
- [15] E. R. Berger, M. Diehl, and B. Pire, Phys. Lett. B **523**, 265 (2001); B. Pire and L. Szymanowski, Phys. Lett. B **622**, 83 (2005); J. P. Lansberg, B. Pire, and L. Szymanowski, Phys. Rev. D **76**, 111502(R) (2007).
- [16] S. Kumano, M. Strikman, and K. Sudoh, Phys. Rev. D **80**, 074003 (2009).
- [17] H. Terazawa, Rev. Mod. Phys. **45**, 615 (1973); S. Cooper, Ann. Rev. Nuc. Part. Sci. **38**, 705 (1988); S. Uehara, Nucl. Phys. B (Proc. Suppl.) **225-227**, 126 (2012).
- [18] A. Freund and M. McDermott, Eur. Phys. J. C **23**, 651 (2002).
- [19] $P = (p + p')/2$ is often used in the GPDs and the same notation P is used in the GDA with the definition $P = p + p'$. In order to distinguish them, $\bar{P} = (p + p')/2$ is used in this article.
- [20] D. Müller, D. Robaschik, B. Geyer, F.-M. Dittes, and J. Horejsi, Fortschr. Phys. **42**, 101 (1994) (hep-ph/9812448).
- [21] M. Diehl, T. Gousset, and B. Pire, Phys. Rev. Lett. **81**, 1782 (1998); Phys. Rev. D **62**, 073014 (2000).
- [22] I. V. Anikin, B. Pire, and O. V. Teryaev, Phys. Rev. D **69**, 014018 (2004); Phys. Lett. B **626**, 86 (2005).
- [23] A. Freund, Phys. Rev. D **61**, 074010 (2000).
- [24] M. Diehl, V. Guzey, and A. Radyushkin, personal communications (2012).
- [25] S. Uehara, personal communications (2013).
- [26] R. Devenish and A. Cooper-Sarkar, Appendix C in *Deep Inelastic Scattering* (Oxford University press, 2004).
- [27] M. Vanderhaeghen, P. A. M. Guichon, and M. Guidal, Phys. Rev. D **60**, 094017 (1999), M. Guidal, M. V. Polyakov, A. V. Radyushkin, and M. Vanderhaeghen, Phys. Rev. D **72**, 054013 (2005); V. Guzey, C. Weiss, talks at the GPD working group mini-workshop, JLab, Aug. 6-7, 2008.
- [28] A. V. Radyushkin, arXiv:hep-ph/0101225, *At the frontier of particle physics : handbook of QCD*, edited by M. Shifman (World Scientific, 2001), Vol.2, pp.1038-1099. See also Ref. [13].
- [29] S. D. Drell and T.-M. Yan, Phys. Rev. Lett. **24**, 181 (1970); G. B. West, Phys. Rev. Lett. **24**, 1206 (1970).
- [30] W. Melnitchouk, R. Ent, and C. E. Keppel, Phys. Rept. **406**, 127 (2005).
- [31] G. R. Farrar and D. R. Jackson, Phys. Rev. Lett. **43**, 246 (1979); A. V. Efremov and A. V. Radyushkin, Theor. Math. Phys. **42**, 97 (1980); A. Duncan and A. H. Mueller, Phys. Rev. D **21**, 1636 (1980); Phys. Lett. **93B**, 119 (1980); G. P. Lepage and S. J. Brodsky, Phys. Rev. D **22**, 2157 (1980).
- [32] G. F. Farrar and D. R. Jackson, Phys. Rev. Lett. **35**, 1416 (1975); S. J. Brodsky, M. Burkardt, and I. Schmidt, Nucl. Phys. B **441**, 197 (1995).
- [33] M. Miyama and S. Kumano, Comput. Phys. Commun. **94**, 185 (1996); M. Hirai *et al.*, Comput. Phys. Commun. **108** (1998) 38; **111**, 150 (1998); **183**, 1002 (2012).
- [34] M. Aicher, A. Schäfer, and W. Vogelsang, Phys. Rev. Lett. **105** (2010) 252003. The PDF code was supplied by W. Vogelsang.
- [35] A. D. Martin, R. G. Roberts, and W. J. Stirling, Phys. Lett. B **636**, 259 (2006).
- [36] B. Povh, K. Rith, C. Scholz, and F. Zetsche, *Particle and Nuclei* (Springer, 1999); D. C. Cheng and G. K. O'Neil, *Elementary Particle Physics* (Addison-Wesley, 1979).
- [37] J. Beringer *et al.* (Particle Data Group), Phys. Rev. D **86**, 010001 (2012); online page <http://ccwww.kek.jp/pdg/>.
- [38] W.-C. Chang, J.-C. Peng, S. Sawada *et al.*, An experimental proposal is under investigation for J-PARC.
- [39] B. Pire and L. Szymanowski, Phys. Lett. B **556**, 129 (2003).
- [40] M. Diehl, T. Feldmann, P. Kroll, and C. Vogt, Phys. Rev. D **61**, 074029 (2000); M. V. Polyakov, Nucl. Phys. B **555**, 231 (1999); M. V. Polyakov and C. Weiss, Phys. Rev. D **60**, 114017 (1999).
- [41] J. F. Donoghue and H. Leutwyler, Z. Phys. C **52**, 343 (1991); X.-D. Ji, Phys. Rev. Lett. **78**, 610 (1997); M. V. Polyakov, Phys. Lett. B **555** 57 (2003); H.-C. Kim, P. Schweitzer, and U. Yakhshiev, Phys. Lett. B **718**, 625 (2012).
- [42] S. J. Brodsky and B. T. Chertok, Phys. Rev. D **14**, 3003 (1976).